2018 Spring Technical Meeting
Central States Section of The Combustion Institute
May 20–22, 2018
Minneapolis, Minnesota

Exit Flow Field of Methane-Fueled Rotating Detonation Engine Measured by Time-Resolved Particle Image Velocimetry

D. Depperschmidt, C. Welch, R. Miller, J. Tobias, M. Uddi, and A. K. Agrawal

Mechanical Engineering, the University of Alabama
Tuscaloosa, AL, USA; aagrawal@eng.ua.edu

Abstract: Pressure gain combustion (PGC) seeks to convert fuel's chemical energy simultaneously into thermal energy and mechanical energy, thereby reducing the entropy production in the process. Recent research has shown that the rotating detonation combustion or combustor (RDC) can provide excellent specific thrust, specific impulse, and large pressure gain through rapid energy release by continuous detonation in the circumferential direction. However, few past studies have employed fuels relevant to power generation gas turbines, since RDC research has focused mainly on aerospace applications. In this study, we present experimental results from RDC operated on methane and oxygen-enriched air to represent reactants used in gas turbines for land-based power generation. The RDC is operated at high pressures by placing a back-pressure plate downstream of the annular combustor. We apply time-resolved particle image velocimetry (PIV) technique, for the first time, to quantify the RDC exit flow at framing rate of 30 kHz. Results show that even though the exit flow is dominantly axial, a significant circumferential velocity component is also present, highlighting the need to condition the flow between RDE exit and turbine inlet. The flow field undergoes cyclic fluctuations, and the key features of the flow field repeat during each cycle. Interestingly, the circumferential velocity shows a reversal in the direction during the cyclic process. Results also show noticeable cycle-to-cycle variations, related to changes in the detonation wave speed, ultimately caused by the rapid fuel-air mixing process at the RDC inlet prior to detonation.

Keywords: Pressure gain combustion, rotating detonation engine, particle image velocimetry

1. Introduction

In an ideal Brayton cycle, combustion occurs at a constant pressure, although in practice the pressure decreases across the combustor by up to about 5%. However, if the same amount of heat is released at constant volume, a much higher temperature with consequent rise in pressure is achieved. This latter approach reduces entropy production during combustion and is referred to as pressure gain combustion (PGC). The idea of capturing available energy from PGC is well recognized, and in fact reciprocating piston engines already involve this principle. One method to achieve PGC for gas turbines is through aerodynamically controlled pulse combustion. NASA Glenn has demonstrated small turbine operation with pressure-gain using pulse combustion [Paxton and Dougherty, 2008]. In another development, a wave rotor PGC relying upon rapid flame propagation has been developed by Roll Royce and collaborators [Akbari and Nalim, 2009].

A simple method to achieve PGC is through detonation where the combustion reaction itself causes the pressure gain. Pulse detonation engine (PDE) provides a robust method to generate

detonation, but does so intermittently at a frequency of about 100 Hz, limited by the reactant fill, fire, and purge sequence. Each cycle in PDE requires ignition, and a long combustion chamber is required to undergo deflagration wave to detonation wave transition (DDT). PDE was demonstrated as a viable combustion device experimentally in laboratory and flight tests [Fernelius et al., 2013]. In 2008, the Air Force Research Laboratory at Wright Patterson Air Force Base used a PDE to propel an aircraft [Barr, 2008]. General Electric has developed a hybrid turbine system with an eight-tube PDE configuration integrated with a single-stage axial turbine. The system operated for up to 5 minutes, and the turbine performance for steady flow operation and with pulsed flow at 20 Hz per tube was similar [Tangarila et al., 2007].

Perhaps, the most significant advance in practical implementation of detonation is the rotating detonation wave combustor or rotating detonation combustion (RDC) based rotating detonation engine (RDE). RDE uses one or more detonation waves that travel circumferentially in an annular chamber for energy conversion as the combustion gas flows downstream axially. Figure 1(a) shows a simple configuration of the RDE. An unwrapped sketch of the RDE taken from Lu and Braun [2014] is shown in Fig. 1(b) to illustrate the key features of the flow and combustion processes. Reactants are injected at left in Fig. 1(a) and at the bottom in Fig. 1(b), mixing rapidly upon injection. Behind the detonation wave, the pressure rises, shutting off the reactant flow until such point that the reactant inflow pressure exceeds the downstream pressure (behind the detonation wave). Subsequently, the reactant injection resumes yielding a triangular shape of mixed, unburned reactants in the annulus to be consumed by the next arrival of the detonation wave. A complex wave interaction is set up depending upon the injector geometry, and properties of the reactants and products. After an initial deflagration to detonation transition, the RDE achieves a quasi-steady periodic state in which fresh reactants enter behind the detonation wave, and product gases expand out the exit plane. While the detonation wave moves circumferentially at a very high speed (in the range of 1.5 to 3.0 km/s), the gas flow is mainly in the axial direction with some swirl component.

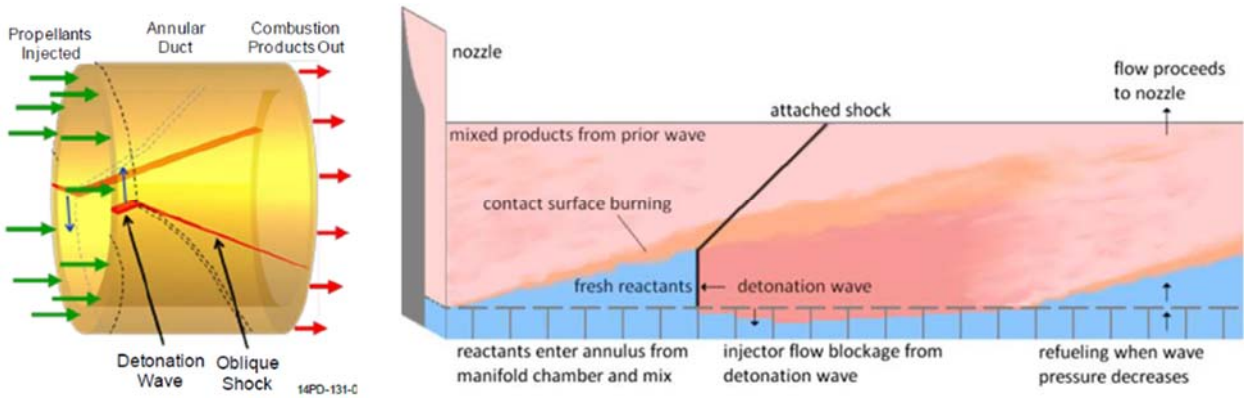

Fig. 1(a) Schematic of an RDE on left [Sonwane et al., 2014], 1(b) RDE wave structure on right [Lu and Braun, 2014].

RDE combustion offers many advantages over conventional detonation engines, such as excellent specific thrust, specific impulse, or specific fuel consumption resulting from rapid energy release of the detonation waveform continuously in the circumferential direction. Quasi-steady detonation in RDE produces exhaust in 1 to 10 kHz frequency range, depending upon the reactant composition, flow rates, equivalence ratio, and geometry of the RDE. RDE relies on inlet manifold pressure to control the flow of fuel and oxidizer into the combustion chamber. Thus, reactant

injection schemes that reduce pressure losses and prevent backflow into the supply plenums are important design issues The effect of the high-frequency periodic flow on turbine performance, efficiency, and durability are largely unknown. It would be desirable to reduce or even eliminate the periodicity observed in the RDC exhaust before the flow enters any power or propulsion devices positioned downstream [Rankin et al., 2014]. Although progress in bringing RDE towards real applications has been substantial in the past few years, challenges remain in efficiently converting detonation energy to useful work. Thus, building upon the unique experiences of Aerojet-Rocketdyne (AR) with RDC design and operation, we are focusing on integration issues of the RDE with power generating gas turbines. Detailed measurements of the 3D flow field at the RDE exit will be necessary to develop strategies to integrate RDE with turbine components located downstream.

In this study, we investigate RDE using methane fuel. Most combined cycle gas turbines operate on natural gas containing methane as the primary fuel constituent. Oxygen-enriched air is used since methane cannot be detonated easily in an RDE using ambient air. First, we demonstrate reliable and reproducible RDE operation with methane and oxygen-enriched air to compliment published RDE studies that have focused mainly on propulsion applications using fuels such as hydrogen or ethylene. Next, we characterize the unsteady flow field at the RDE exit to determine the expected turbine inlet conditions. Time-resolved particle image velocimetry (PIV) technique will be utilized to measure temporally and spatially resolved flow field with the purpose of quantifying the RDE exit flow, which is necessary to identify, understand, and address critical turbine integration issues. The RDE is operated at a high pressure by constraining the exit flow by a back-pressure plate and thus, to more realistically replicate the turbine inlet conditions, thereby maintaining the pressure gain. Experiments seek to provide essential test data to help validate and calibrate the concurrent numerical studies.

2. Methods / Experimental

Figure 2 shows the schematic diagram and a photograph of the RDC in the Engine and Combustion Laboratory (ECL) at the University of Alabama. The annular combustion chamber has an outer diameter of 10.0 cm, inside diameter of 8.0 cm, and height of 13.9 cm. The combustor is made of three concentric rings and a circular center-body that extend into a nose cone above the rings. Another ring with converging-diverging nozzle profile on the inside is placed above the three RDC rings to replicate the back pressure effects of flow conditioning devices when integrating the RDE with the turbine inlet. The RDE sits atop an injector plate with discrete holes to introduce fuel and oxidizer into the combustor annulus through a circular manifold assembly. The RDE components are made of copper and all of the circular rings are connected together by through-bolts screwed into tapped holes attached to the adjustable feet that are secured to the ground by an anchored plate.

An intricate flow system was designed to regulate and deliver the reactants at high flow rates during the experiments. This system consists of three separate areas: gas storage, control panel, and test stand, each designed to fulfill various requirements of the experiment. Gas storage area is located outside the test cell, and it consists of multiple compressed gas cylinders connected through custom-designed manifolds for each supply gas; air, oxygen, and methane for the RDC and hydrogen and oxygen for the pre-detonation chamber. Prior to the experiment, fast acting electro-pneumatic (EP) valves are used to pressurize the line between the compressed gas cylinders and

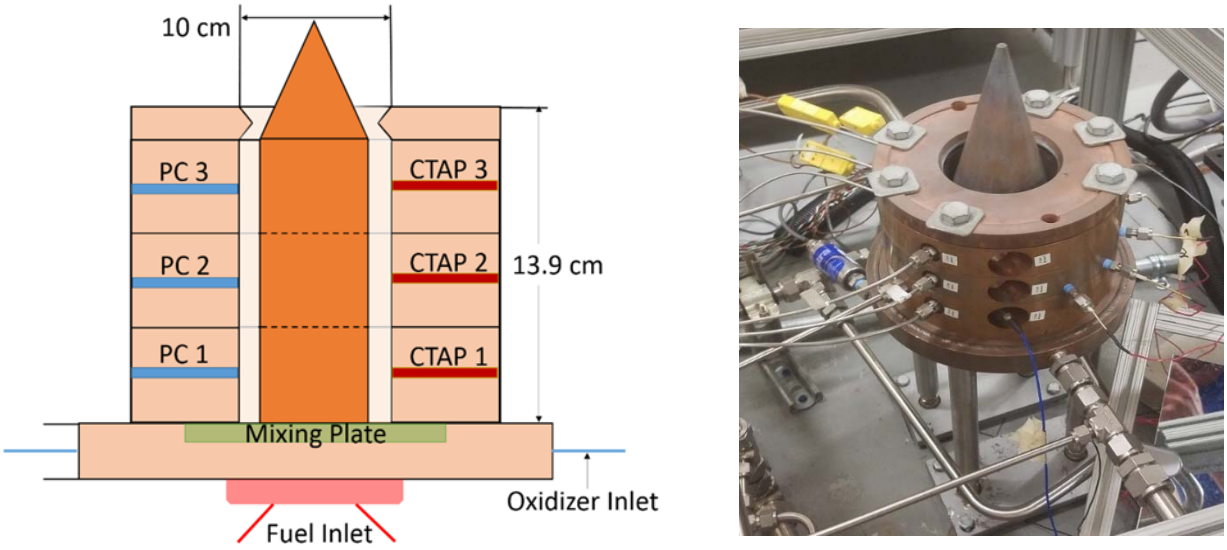

Figure 2. (a) Schematic diagram, and (b) Photograph of the RDE at University of Alabama

the control panel. The control panel itself is located inside the test cell but about 2 meters away from the test section to avoid direct exposure to high temperatures. For each gas supply, the control panel consists of a nitrogen fed dome-loaded regulator and a sonic nozzle assembly with upstream and downstream condition tubes containing pressure and temperature transducers to determine the flow rate. The test section area includes a second set of fast acting electro-pneumatic (EP) valves to actuate the main flow, and solenoid valves to supply the hydrogen and oxygen to the pre-detonator tube. A combustion wave ignitor (CWI) is used to initiate the detonation in the RDE. A stoichiometric mixture of hydrogen and oxygen is supplied to the detonation tube and ignited at the closed upstream end via an automotive spark plug. The ignited mixture undergoes DDT in the detonation tube and the resulting detonation wave is introduced into the combustor through an opening in the wall of the first RDE ring. The control panel includes CWI components such as ball valves and sonic nozzle assemblies with pressure and temperature transducers to measure the hydrogen and oxygen flow rates. The test section area includes CWI components such as solenoid valves, check valves, ignition system, and the detonation tube (Tobias, et. al., 2018).

Pressure across each sonic nozzle is measured by absolute pressure transducers (Lord Sensing and Setra ASM) with measurement error and uncertainty less than 1%. The pressure upstream of the injector plate is measured in the fuel and air manifolds by Setra ASM transducers mounted on 3.18 mm diameter, 15.24 cm extension tubes to dampen the pressure fluctuations. Likewise, the capillary tube average pressure (CTAP) static ports and pressure capillary (PC) static ports are located on each of the three combustor rings, flush with the inner wall of the ring. Pressure is measured by SETRA transducers mounted at the end of the 3.18 mm diameter, 45.22 cm long tube for CTAP and 3.18 mm diameter and 15.24 cm long tube for PC ports. Additionally, four ion-probes separated circumferentially by 25° are mounted on ring two. Probe measurements are acquired by a National Instruments cDAQ 9172 chassis operated via LabVIEW. The chassis contains multiple modules for data acquisition at high (1 MHz) and low (1 kHz) speeds (Cooper et al, 2018).

The combustion event is visualized by multiple high-speed digital cameras as illustrated in Figure 3. The detonation wave is visualized directly by a color camera (Photron SA-5) with a 50-600 mm zoom lens. The camera is positioned on a tripod at a safe distance away from the RDE

and it views the inside of the RDE through a set of two precisely aligned adjustable mirrors. The first mirror is located in the exhaust hood ceiling above the RDE. The second mirror is placed near the ground to re-directs the image to the high-speed camera. The optical path length between the RDE base and camera is about 4 meters. This arrangement yields images of the detonation wave at the base on the RDC at 186,000 frames per second (fps) and 192x144 pixel size. The combustor exhaust is visualized by another high-speed color camera (Photron SA-5) at pixel resolution of 192 x 746 and frame rate of 30,000 fps, designated as the "low-speed" camera. Without detonation, the spectral intensity of the exhaust flow is reduced dramatically, and hence, a longer exposure time (or smaller frame rate) is necessary to acquire acceptable quality images of the exhaust flow. Again, the camera is placed on a tripod at a safe distance away from RDC.

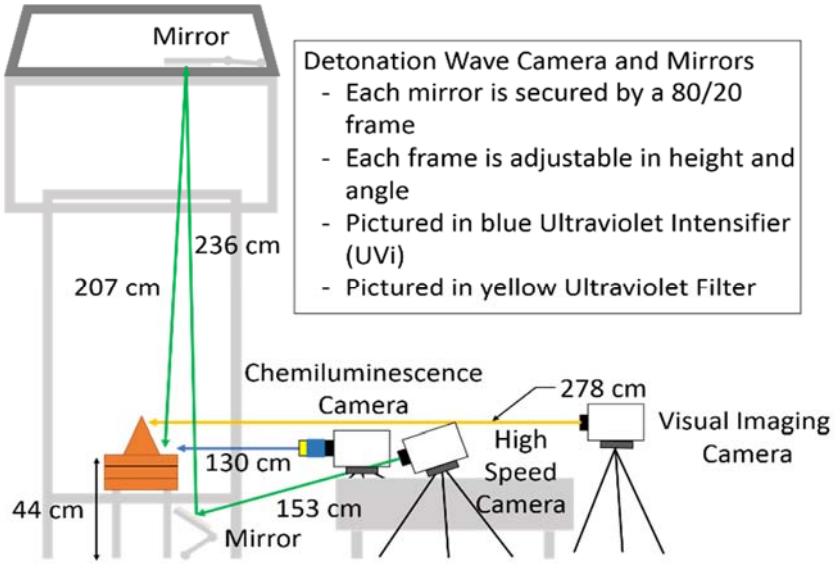

Figure 3. Arrangement of high-speed camera systems for different measurements of the RDE.

The flow field is measured by a time-resolved particle image velocimetry (PIV) system. The diagnostics hardware include a Quantronix Hawk Duo 120 watt, 532 nm Nd-YAG laser, Photron SA-5 high-speed camera, and a synchronizer. The camera is positioned away from the central axis of the RDE. As shown in Figure 4, the image size is about 300x300 pixels, and field of view is 29.09 mm by 29.09 mm, resulting in spatial resolution of about 100 µm per pixel. The time between the two laser pulses, commonly referred to as the Δt, was set to 1 µs, while the camera operated at 60,000 frames per second (fps). This frame rate yielded PIV images at 30,000 Hz since each PIV image requires two consecutive camera frames. Instantaneous velocity vector plots were calculated within the TSI Insight 4G software, and analyzed in Tecplot Focus to observe cyclical behavior of the hydrodynamic structures within the flow field.

A seeder system was designed and developed for this study. The seeder operated on a separate air supply line, and the seeded airflow is injected into the main oxidizer flow line upstream of the RDE manifold. Several different seed particles were attempted, which led to the selection of 200 nm diameter zirconium oxide particles for the final experiments. A typical run consumed just a few grams of the seed particles. The timing of the seed particle with respect to the remaining flow lines is important, and was optimized based on multiple trial experiments.

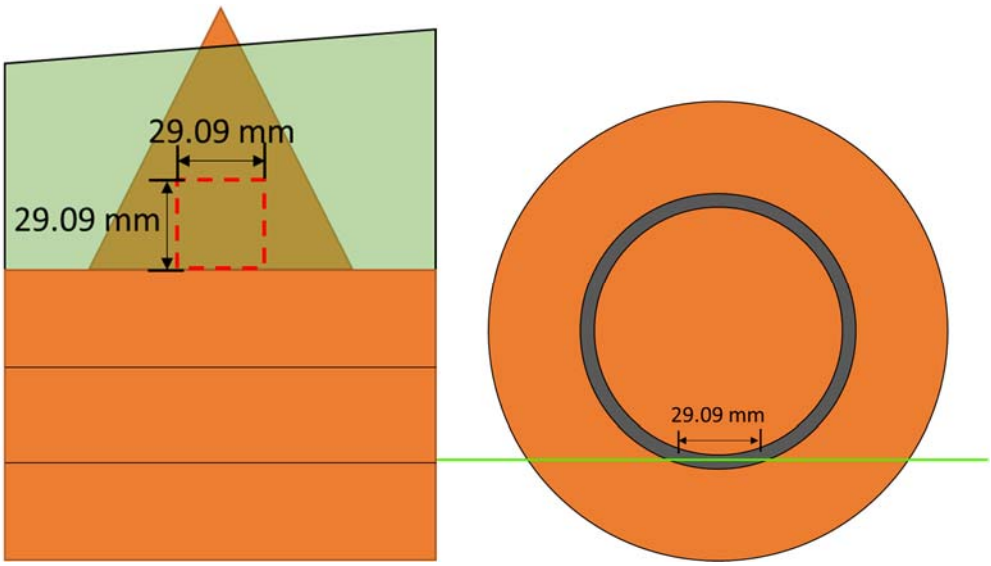

Figure 4. Illustration of the PIV measurement window/plane at the exit of RDE.

The timing of the experiment is controlled precisely via two BeagleBone Black microcontrollers. A controller outside of the test cell opens normally closed EP valves located downstream of the main gas manifolds. A microcontroller inside of the test cell controls the initiation of the experimental sequence via a secured shell connection to the first microcontroller by actuating EP valves and solenoid valves, triggering low-speed DAQ, high-speed DAQ, and high-speed digital cameras. Prior to the test sequence, all gas lines are pressurized and the pressure on each pressure regulator on the control panel is set to obtain the desired flow rate flow. EP and solenoid valves are timed precisely to prevent reactants from burning in the deflagration mode. DAQ and high-speed imaging systems are turned-on prior to the ignition event. For safety reasons, the fuel flow is turned on last before ignition and turned-off first after ignition. A nitrogen purge system is used to purge all lines before and after the test.

3. Results and Discussion

Time-Resolved PIV Measurements

Figure 5 shows the instantaneous velocity vector fields during a cycle. Portions of select flow fields are not resolved with velocity vectors due to factors such as insufficient seed density and/or distribution, or insufficient laser intensity/light scattering. The scale of the velocity magnitudes, though hard to read, shows that the red vectors correspond to 2,000 m/s, orange approximately 1,666.67 m/s, green 1,000 m/s, and dark blue 333.33 m/s. Several interesting observations are made: the flow is highly unsteady or time-dependent, the flow direction is mainly axial, but significant circumferential flow is also present, the circumferential flow direction changes during the cycle, and significant cycle-to-cycle variations in the flow field can be observed.

To better quantify the variations in axial and circumferential velocities observed, individual discrete points in the flow field were selected to create the scatter plot shown in Figure 6. The points selected for these plots are along centerline of the image, 4.36 mm downstream of the RDE

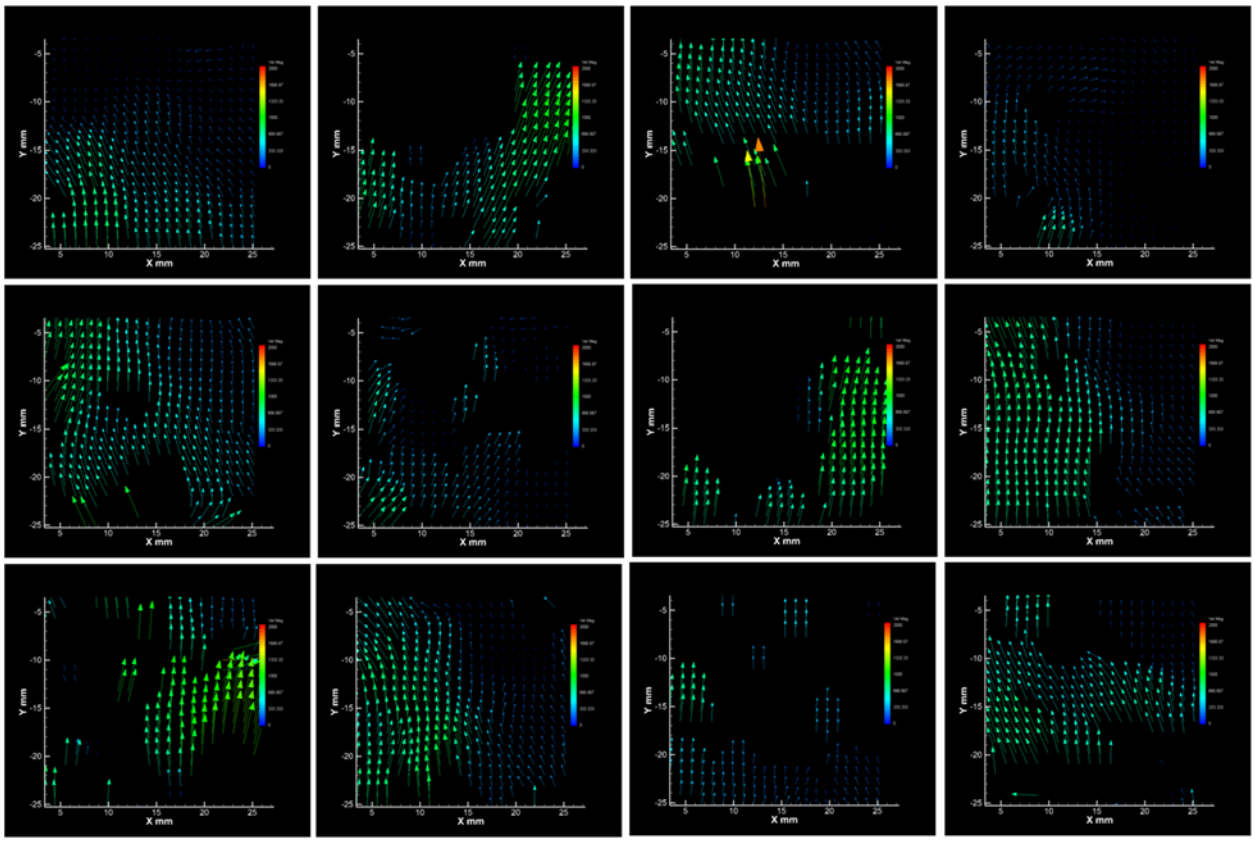

Figure 5. Processed instantaneous PIV resolved velocity vector flow fields downstream of the RDE; images are arranged sequentially from top to bottom, left to right.

exit (Figure 6a, 6b) and 2.91 mm downstream of the exit (Figure 6c, 6d). Approximately 800 consecutive PIV image pairs were analyzed representing time span of 25 ms. Few key observations are made from these scatter plots: The axial remains positive through the selected data sequence, and generally ranges from 0 to 1000 m/s, while some values were calculated to be as high as 2000 m/s. These extreme velocity calculations are subject to greater uncertainty, which remains to be specifically quantified. However, the circumferential velocity components range from both negative (CW) and positive (CCW) values, varying generally from -400 m/s to 500 m/s.

Next, data in Figure 6 are used to generate histograms of the axial and circumferential velocities displayed in Figure 7. It should be noted that the total number of data points is less than the 800 PIV image pairs since some of the pairs did not resolve velocity values at the specified point in the flow field. It can be seen from these histogram plots that the median velocity for the axial component of the flow is approximately 500 m/s, while the distribution of values is generally asymmetric with velocities less than 500 m/s occurring more frequently than those greater than 500 m/s. Axial velocities greater than 2,000 m/s or less than 0 m/s are considered outlier values at this time. The median value for the circumferential velocities was approximately 0 m/s. While the distribution of circumferential velocities is also asymmetric, positive (CCW) values occurred more frequently than negative values. The maximum and minimum circumferential velocities recorded were 500 and -300 m/s, respectively, though outliers were rarely measured.

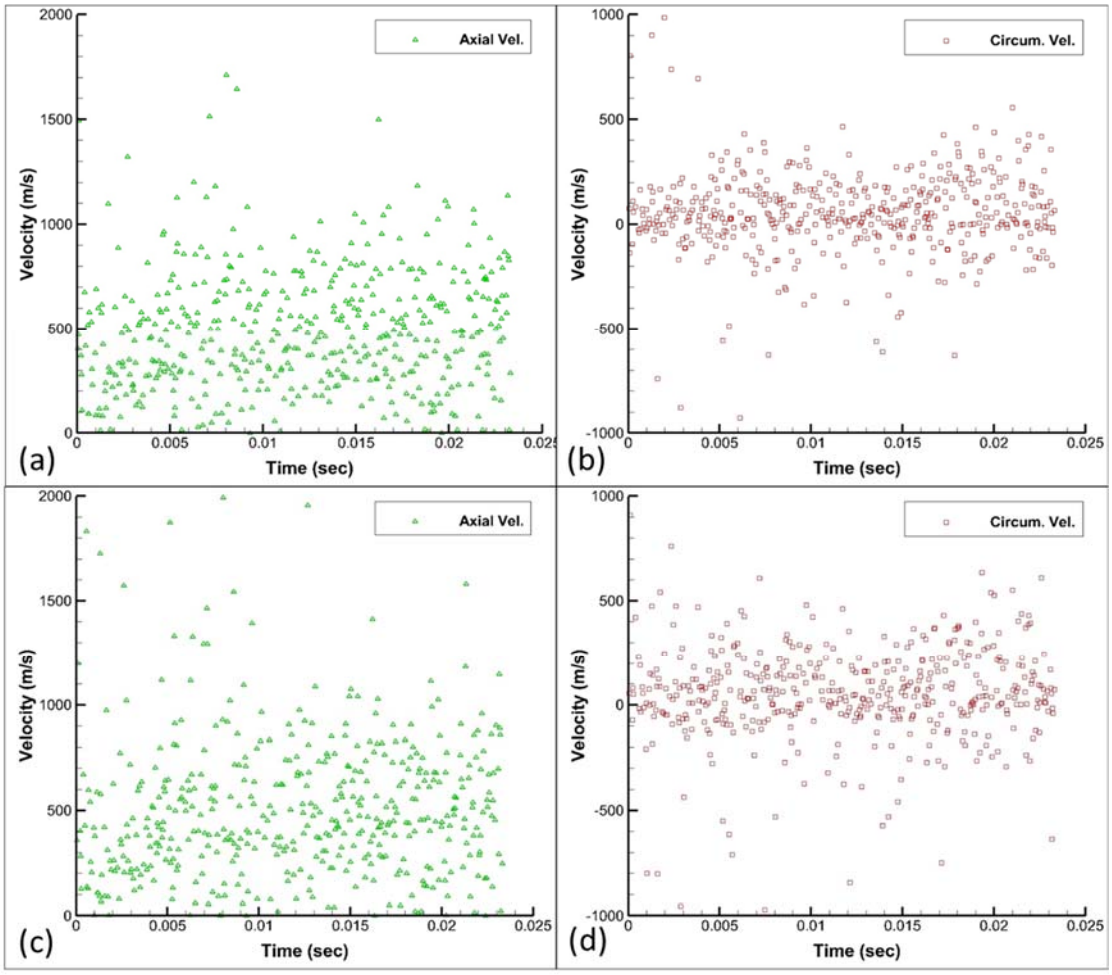

Figure 6. Velocity at the RDE exit (a & b) 4.36 mm downstream of exit and (c & d) 2.91 mm downstream of exit.

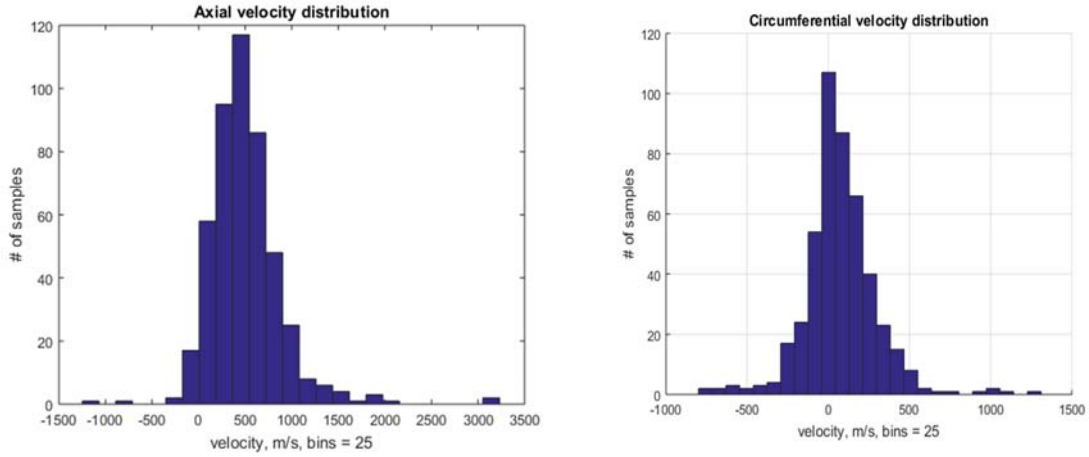

Figure 7. Histogram of the (a) axial velocity (left), and circumferential velocity (right)

4. Conclusions

This study details initial experiments conducted in a rotating detonation engine, operated at a high pressure with methane fuel. The flow field at the exit of the RDE was measured by particle image velocimetry operated at image pair acquisition rate of 30 kHz. The study resulted in the following conclusions:

- The flow field exiting the RDE is highly turbulent and unsteady, and contains shock structures.
- The axial and circumferential velocity components vary significantly during the transient flow.
- The circumferential velocity was found to vary periodically between -300 to 500 m/s.

Multiple steps will be taken in future studies to improve the PIV diagnostics; including higher seeder flow rate and supply pressure, higher laser pulse energy, shorter laser pulse duration, etc., to improve the measurement uncertainties. Additionally, PIV measurements will be coupled with high frequency diagnostics such as dynamic pressure probes to create an ensemble average of how both axial and circumferential velocities vary within a cycle.

5. Acknowledgements

This material is based upon work supported by the Department of Energy under Award Number(s) DE-FE0023983."

References

1. Akbari, P., and Nalim, R., “Review of recent developments in wave rotor combustion technology,” *Journal of Propulsion and Power*, Vol. 25, 2009, pp. 833-844.
2. Barr, L., *Pulsed Detonation Engine Flies into History*, May 2008.
3. Fernelius, M.H., Gorrell, S.E., Hoke, J.L., and Schauer, F.R., “Design and Fabrication of an Experimental Test Facility to Compare Performance of Pulsed and Steady Flow through a Turbine,” AIAA Paper 2013-0277.
4. Lu, F.K., and Braun, E.M., “Rotating Detonation Wave Propulsion: Experimental Challenges, Modeling, and Engine Concepts,” *Journal of Propulsion and Power*, Vol. 30, No. 5, 2014, pp. 1125-1142.
5. Paxson, D.E., et al., “Comparison of Numerically Simulated and Experimentally Measured Performance of a Rotating Detonation Engine,” AIAA Paper 2015-1101.
6. Rankin, B.A., Hoke, J.L., and Schauer, F.R., “Periodic Exhaust Flow through a Converging-Diverging Nozzle Downstream of a Rotating Detonation Engine,” AIAA Paper 2014-1015.
7. Schwer, D.A., and Kailasanath, K, “Physics of Heat-Release in Rotating Detonation Engines,” AIAA Paper 2015-1602.

8. Sonwane, C., Claflin, S., Lynch, E.D., Stout, J., “Recent Advances in Power Cycles Using Rotating Detonation Engines with Subcritical and Supercritical CO_2” Proceedings of the 4th International Symposium - Supercritical CO2 Power Cycle, Pittsburgh, Pennsylvania, September 2014.
9. Tangirala, V., Rasheed, A., and Dean, A.J., “Performance of a Pulse Detonation Combustor-Based Hybrid Engine” ASME Paper GT 2007-28056.
10. C. Welch, D. Depperschmidt, R. Miller, J. Tobias, M. Uddi, and A. K. Agrawal, and Lowe, S., 2018, Experimental Analysis Of Wave Propagation In A Methane-Fueled Rotating Detonation Combustor, ASME Paper GT2018-77258.
11. J. Tobias, D. Depperschmidt, R. Miller, C. Welch, M. Uddi, and A. K. Agrawal, and Daniel, R., 2018, “OH* chemiluminescence imaging of the combustion products from a methane-fueled rotating detonation engine,” ASME Paper GT2018-77255.